ACS APPLIED MATERIALS & INTERFACES

Research Article

www.acsami.org

Incorporating Zwitterionic Graphene Oxides into Sodium Alginate Membrane for Efficient Water/Alcohol Separation

Jing Zhao,[†,‡] Yiwei Zhu,[†,‡] Guangwei He,[†,‡] Ruisi Xing,[†,‡] Fusheng Pan,[†,‡] Zhongyi Jiang,*[,†,‡] Peng Zhang,[§,∥] Xingzhong Cao,[§,∥] and Baoyi Wang[§,∥]

[†]Key Laboratory for Green Chemical Technology of Ministry of Education, School of Chemical Engineering and Technology, Tianjin University, Tianjin 300072, China

[‡]Collaborative Innovation Center of Chemical Science and Engineering (Tianjin), Tianjin 300072, China

[§]Multi-discipline Research Division, Institute of High Energy Physics, Chinese Academy of Sciences, Beijing 100049, China

[∥]Beijing Engineering Research Center of Radiographic Techniques and Equipment, Beijing 100049, China

Supporting Information

ABSTRACT: For the selective water-permeation across dense membrane, constructing continuous pathways with high-density ionic groups are of critical significance for the preferential sorption and diffusion of water molecules. In this study, zwitterionic graphene oxides (PSBMA@GO) nanosheets were prepared and incorporated into sodium alginate (SA) membrane for efficient water permeation and water/alcohol separation. The two-dimensional GO provides continuous pathway, while the high-density zwitterionic groups on GO confer electrostatic interaction sites with water molecules, leading to high water affinity and ethanol repellency. The simultaneous optimization of the physical and chemical structures of water transport pathway on zwitterionic GO surface endows the membrane with high-efficiency water permeation. Using dehydration of water/alcohol mixture as the model system, the nanohybrid membranes incorporating PSBMA@GO exhibit much higher separation performance than the SA membrane and the nanohybrid membrane utilizing unmodified GO as filler (with the optimal permeation flux of 2140 g m^{-2} h^{-1}, and separation factor of 1370). The study indicates the great application potential of zwitterionic graphene materials in dense water-permeation membranes and provides a facile approach to constructing efficient water transport pathway in membrane.

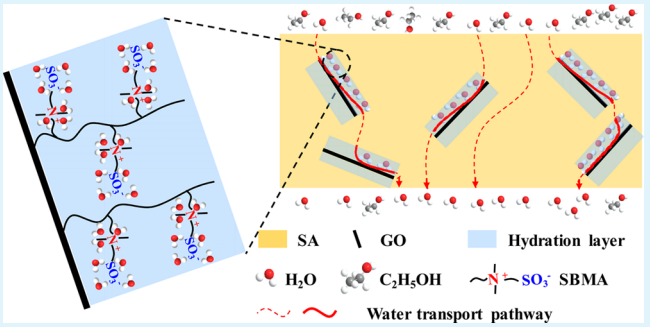

KEYWORDS: *zwitterionic, graphene oxides, nanohybrid membrane, water transport pathway, water/alcohol separation*

INTRODUCTION

The selective water-permeation across dense membrane is a pivotal issue in various membrane processes including pervaporation, vapor permeation, and reverse osmosis, with applications spanning from bioalcohol recovery to water treatment.[1−3] Hydrophilic groups are imperative carriers for water permeation, which comprise ionic/nonionic types, and bind water molecules via electrostatic interaction/hydrogen bond, respectively.[4] Because of the higher bond strength and lower directionality of electrostatic interaction compared with hydrogen bond, the ionic groups are usually conferred with higher water affinity and water uptake,[5] which are favorable for the preferential sorption of water molecules, the initial step of water permeation process. Apart from the type of hydrophilic groups, the group density and distribution are also critical factors for water permeation, because they determine the proximity effect of the neighboring hydrophilic groups and the connectivity of the water transport pathway, exerting great influence on water diffusion,[6] another step of water permeation process. Therefore, constructing continuous pathway with high-density ionic groups in membrane is a viable strategy to acquire high-efficiency water permeation.

Recently, zwitterionic materials possessing moieties with both cationic and anionic groups have emerged as promising superhydrophilic materials.[7−9] Compared with other hydrophilic materials, zwitterionic material has the following advantages: (i) the abundant ionic groups provide affluent electrostatic interaction sites with water molecules, thus inducing denser and stronger hydration layer, and leading to higher repellency against competitive molecules;[5,8,10] (ii) the water molecules outside the hydration layer of zwitterionic materials possess higher freedom compared with those outside the hydration layer induced by hydrogen bond;[5] (iii) the distinct charge-neutral feature endows zwitterionic monomers with higher reactivity for free radical polymerization compared with other charged monomers because of the increased affinity

Received: November 2, 2015
Accepted: January 5, 2016
Published: January 14, 2016

DOI: 10.1021/acsami.5b10551
ACS Appl. Mater. Interfaces 2016, 8, 2097−2103

between monomers, thus easily obtaining polyzwitterions with high ionic group density.[11,12] All the above features are in favor of the selective water-permeation across membrane. Up to now, a vast number of zwitterionic materials have been exploited with their hydration properties being intensively studied. However, the applications of zwitterionic materials in membrane field mainly focus on the construction of super-hydrophilic membrane surface to form hydration layer and eliminate fouling in porous membranes.[13−16] Their effects on selective water-permeation in dense membranes have rarely been investigated.

In this study, sulfobetaine methacrylate (SBMA) was utilized as the monomer to prepare zwitterionic graphene oxide (GO) nanosheets with high grafting density via free radical polymerization method. SBMA is a representative zwitterionic material possessing quaternary ammonium group with positive charge and sulfonate group with negative charge simultaneously, which are both completely dissociated in water,[17] thus generating abundant electrostatic interaction sites with water molecules. GO is a burgeoning two-dimensional carbon material with one-atom thickness, high aspect ratio, high specific surface area and rich modification approaches.[18] Consequently, the nanohybrid membranes with GO-based fillers can confer continuous transport pathways with chemical diversity on GO surfaces.[19,20]

Herein, polymer-inorganic nanohybrid membranes were fabricated by incorporating zwitterionic GO into sodium alginate (SA) matrix (Figure 1) and utilized for water/alcohol

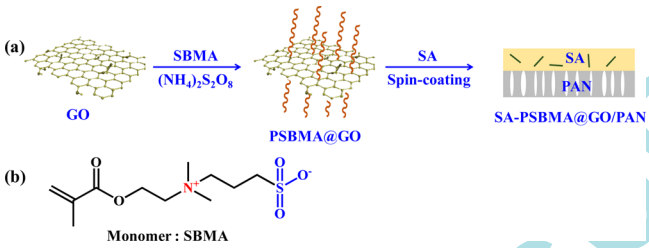

Figure 1. (a) Schematic representation of the membrane fabrication procedure and (b) molecular structure of zwitterionic monomer sulfobetaine methacrylate.

separation. The effects of incorporating continuous zwitterionic pathway on nanohybrid membrane structure and membrane separation performance were investigated.

MATERIALS AND METHODS

Materials. Natural flake graphite (2500 mesh) was received from Qingdao Tianhe Graphite Co. Ltd. (Shandong, China). Hydrochloric acid (HCl, 36−38 wt %), potassium permanganate ($KMnO_4$) and sulfuric acid (H_2SO_4, 98 wt %) were purchased from Tianjin Kewei Ltd. (Tianjin, China). Sodium nitrate ($NaNO_3$), hydrogen peroxide aqueous solution (H_2O_2, 30 wt %), ethanol (≥99.7 wt %), *N*,*N*-dimethylformamide (DMF, ≥ 99.9 wt %), sodium hydroxide (NaOH), and calcium chloride ($CaCl_2$) were supplied by Tianjin Guangfu Fine Chemical Research Institute (Tianjin, China). Ammonium peroxydisulfate ($(NH_4)_2S_2O_8$, 99.99 wt %) was supplied by Shanghai Aladdin Biochemical Technology Co., Ltd. (Shanghai, China). Sulfobetaine methacrylate (97 wt %) was purchased from Sigma-Aldrich (USA). Sodium alginate (SA) was received from Qingdao Bright Moon Seaweed Group Co. Ltd. (Shandong, China). The polyacrylonitrile (PAN) ultrafiltration membrane (molecular weight cutoff: 100 kDa) with the flat-sheet configuration was purchased from Shandong MegaVision Membrane Technology & Engineering Co. Ltd. (Shandong, China). All chemicals used were in analytical grade. Deionized water was utilized in all of the experiments.

Preparation of Zwitterionic Graphene Oxides. Zwitterionic graphene oxides were prepared via free radical polymerization method.[21,22] First, GO dispersion was prepared following the modified Hummers method as described in our previous study.[23] Afterward, 40 mL of GO dispersion (2.5 mg mL^{-1} with water as solvent) and 90 mL of DMF were added into a flask and sonicated for 30 min. Then, 50 mL of SBMA aqueous solution (60 mg mL^{-1}) was added into the GO dispersion and stirred for 30 min with the flask in a thermostated oil bath at 60 °C. One hundred milliliters of $(NH_4)_2S_2O_8$ aqueous solution (1.2 mg mL^{-1}) was prepared and added dropwise through a constant pressure funnel after the solution was purged under nitrogen for 30 min. The reaction mixture was stirred at 60 °C under nitrogen for 40 h. After that, the mixture was cooled to room temperature, diluted with 400 mL of water, sonicated for 1 h, and washed with water and ethanol. The obtained precipitates after centrifugation were zwitterionic GO, designated as PSBMA@GO.

Fabrication of Nanohybrid Membranes. The nanohybrid membranes were fabricated via spin-coating method. First, the removal of glycerin from the PAN membrane was achieved by immersing it in water for 48 h, and then the membrane was fixed on spin coater after fully dried. Meanwhile, PSBMA@GO aqueous dispersion was prepared and sonicated for 1 h. After sonication, SA was added and stirred for 4 h at 30 °C to obtain a homogeneous SA-PSBMA@GO casting solution. The SA concentrations were 1.5 wt % for all the membranes, while the mass ratio of PSBMA@GO to SA varied from 0 wt % to 7.5 wt %. After filtrated and kept still for several minutes to remove air bubbles, the SA-PSBMA@GO casting solutions were spin-coated on PAN ultrafiltration membranes and dried at room temperature. Finally, the as-fabricated nanohybrid membranes were soaked in a 0.5 M $CaCl_2$ solution for 10 min, then rinsed with deionized water and dried at room temperature. The obtained membranes were named as SA-PSBMA@GO(X)/PAN, in which X was the mass ratio of PSBMA@GO to SA. Meanwhile, the homogeneous membranes were prepared for characterization by casting the same solutions on glass plates and named as SA-PSBMA@GO(X). For comparison, the membrane with pristine GO as filler was fabricated and named as SA-GO(Y)/PAN, in which Y was the GO/SA mass ratio.

Membrane Characterizations. The morphology of PSBMA@GO was observed by transmission electron microscopy (TEM, JEOL JEM-100CXII) and atomic force microscope (AFM, CSPM 5000). Element mapping equipped on TEM was employed to characterize the element distribution on PSBMA@GO. FTIR spectra with a scan range of 2500−450 cm^{-1} were measured using BRUKER Vertex 70 FT-IR spectrometer. The chemical compositions of pristine and zwitterionic GO were measured by X-ray photoelectron spectroscopy (XPS, Kratos Axis Ultra DLD) with a monochromatic Al Kα source and a charge neutralizer to ascertain the successful grafting of PSBMA. The measurement of static water contact angles was performed using a contact angle goniometer (JC2000C Contact Angle Meter) to evaluate the hydrophilicity of GO and PSBMA@GO. Field emission scanning electron microscope (FESEM) (Nanosem 430) was utilized to observe the cross-section and surface morphologies of membranes. To acquire the thermal properties of GO and PSBMA@GO, thermogravimetric analysis (TGA, NETZSCH TG 209 F3) was used heating from 40 to 800 °C (rate = 10 °C min^{-1}) in N_2 atmosphere. The free volume properties of membranes was analyzed by positron annihilation lifetime spectroscopy (PALS) using an EG&G ORTEC fast−slow coincidence system with a resolution of 208 ps. The positron source (22Na, 13 μci) was sandwiched between two pieces of samples with size of 1 cm × 1 cm and thickness of approximately 0.5 mm. A semiempirical equation given by eq 1 correlates o-Ps annihilation lifetime (τ_3 and τ_4) with the radius of the free volume cavity, r_3 and r_4 (Δr = 0.1656 nm).[24]

$$\tau = \frac{1}{2}\left[1 - \frac{r}{r + \Delta r} + \left(\frac{1}{2\pi}\right)\sin\left(\frac{2\pi r}{r + \Delta r}\right)\right]^{-1} \quad (1)$$

DOI: 10.1021/acsami.5b10551
ACS Appl. Mater. Interfaces 2016, 8, 2097−2103

The apparent fractional free volume (f_{app}) of membranes could be calculated with the following equation (I is the annihilation intensity of o-Ps):

$$f_{app} = \frac{4}{3}\pi(r_3^3 I_3 + r_4^3 I_4) \quad (2)$$

Membrane Separation Experiments. The pervaporation separation of water/ethanol mixture was utilized to evaluate the performance of nanohybrid membranes for selective water-permeation.

Pervaporation experiments were performed with a P-28 membrane module (CM-Celfa AG Company, Switzerland).[3] The downstream pressure of membrane was kept below 0.3 kPa with a vacuum pump, and the flow rate of feed solution was controlled at 60 L h^{-1}. The permeate was collected with a liquid nitrogen cold trap after the membrane reached steady state. The permeate solution was weighed. Gas chromatography (Agilent 7820A, USA) was utilized to analyze the compositions of feed and permeate solutions. The permeation flux (J, g m^{-2} h^{-1})), separation factor (α) and pervaporation separation index (PSI) of the membranes are calculated through the equations as follows:

$$J = \frac{Q}{A \times t} \quad (3)$$

$$\alpha = \frac{P_W/P_E}{F_W/F_E} \quad (4)$$

$$\mathrm{PSI} = J \times (\alpha - 1) \quad (5)$$

where Q represents the mass of collected permeate (g), t represents the collection interval (0.5 h), and A represents the actual membrane area contacting with feed (2.56×10^{-3} m^2). P represents the mass fraction of water (subscript W) or ethanol (subscript E) in permeate solution, while F represents the mass fraction of water or ethanol in feed solution. Three membranes were prepared under every condition, and each membrane was measured repeatedly for three times to ensure the reliability of experimental data. The average of multiple results was utilized as the final data.

RESULTS AND DISCUSSION

Morphology and Chemical Structure of PSBMA@GO. The morphology of PSBMA@GO was characterized by TEM and AFM. Compared Figure 2a and b, it can be observed that the transparent and lamellar morphology of GO is preserved after modification, while the transparency decreases because of the covering of PSBMA on GO.[25] Figure 2c–f show the distribution of C, N, and S elements on PSBMA@GO, among which N and S are the characteristic elements of SBMA monomer. Therefore, Figure 2e and f confirm the successful grafting and uniform distribution of PSBMA on GO. The 20 μm × 20 μm AFM image in Figure 2g exhibits the irregular shape and submicrometer-scale size along horizontal direction of PSBMA@GO. The thickness of PSBMA@GO sheets is measured to be about 4.1 nm from the height profile in Figure 2h, which is much higher than that of GO, further demonstrating the success of polymer grafting.[22]

The FT-IR spectra of pristine and zwitterionic GO were obtained as shown in Figure 3a to analyze the chemical structure transformation of GO after modification. Several new adsorption peaks appear on the spectrum of PSBMA@GO at 1720 cm^{-1} because of the stretching vibration of —C═O in ester group, 1170 cm^{-1} due to the asymmetric stretching vibration of O═S═O in sulfonate, and 1036 cm^{-1} due to the stretching vibration of —C—N in quaternary ammonium group, corresponding to the chemical groups on SBMA.[12,15] XPS analysis of GO and PSBMA@GO was performed to obtain

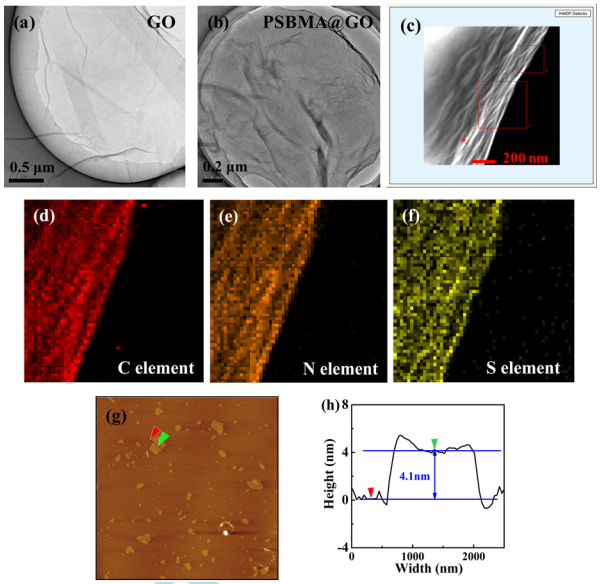

Figure 2. (a) TEM image of GO, (b) TEM image of PSBMA@GO, (c–f) element mapping of PSBMA@GO, (g) AFM image of PSBMA@GO, and (h) height profile of PSBMA@GO.

the grafting amount of PSBMA. As shown in Figure 3c, N 1s, S 2s, and S 2p peaks appear on the spectrum of PSBMA@GO. According to the S element content of 7.66 wt %, the content of PSBMA in PSBMA@GO can be calculated to be 66.79 wt %. Therefore, the grafting amount of PSBMA is 2.01 g g^{-1}, while the grafting density is 1.67 SBMA unit nm^{-2}, which means that there are 3.34 charged groups in the area of one square nanometer. The hydrophilicity of GO and PSBMA@GO was characterized by measuring the water contact angles (Figure 3d). The employed samples are GO and PSBMA@GO membranes fabricated via suction filtration of the corresponding aqueous dispersions. The water contact angle declines from 47.3 ° to 29.4 ° after zwitterionic modification of GO, revealing the significantly improved hydrophilicity, which arises from three reasons. First, the grafting of PSBMA on GO is performed via free radical polymerization, which occurs on the carbon–carbon double bonds of GO instead of the oxygen-containing groups commonly used in other chemical modification.[21,22] Therefore, the original hydrophilic groups on GO are reserved. Second, zwitterionic unit possesses abundant charged groups, which bind water molecules through strong electrostatic interaction, while most of the hydrophilic groups on GO are neutral and bind water molecules through hydrogen bonds. The water molecules adsorbed through electrostatic force are less direction sensitive than those through hydrogen bond. It has been reported that about eight water molecules can be tightly bound with one SBMA unit.[5] Last but not least, the grafting amount of PSBMA is much higher than the original hydrophilic groups on GO. In order to investigate the change of GO's affinity for water and ethanol after modification, both GO and PSBMA@GO dispersions with water and ethanol as solvents were prepared. As shown in Figure S1, GO disperses well both in water and ethanol, while PSBMA@GO precipitates in ethanol, confirming its ethanol repellency arising from the abundant charged groups on PSBMA.

Morphology of Nanohybrid Membranes. According to the grafting amount of PSBMA, the content of GO in SA-

DOI: 10.1021/acsami.5b10551
ACS Appl. Mater. Interfaces 2016, 8, 2097–2103

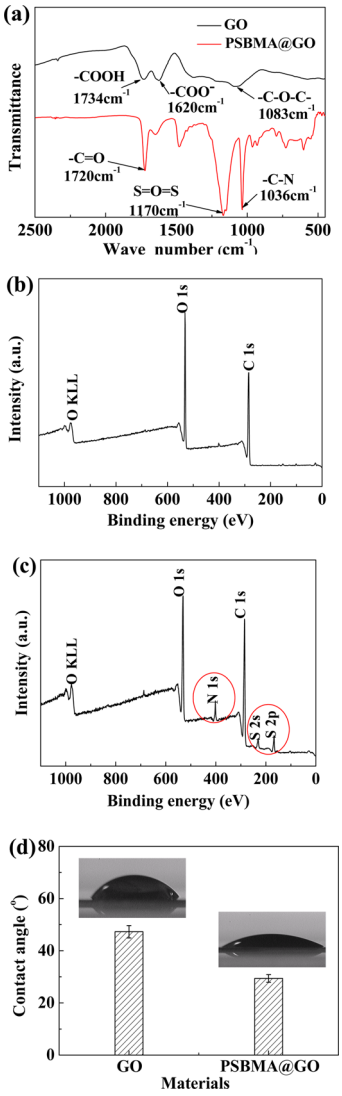

Figure 3. (a) FT-IR spectra of GO and PSBMA@GO, (b) XPS spectrum of GO, (c) XPS spectrum of PSBMA@GO, and (d) water contact angles of GO and PSBMA@GO.

PSBMA@GO(2.5)/PAN membrane is calculated to be about 0.8 wt %. Therefore, the SA-GO(0.8)/PAN and SA-GO(0.8) membranes were fabricated for comparison. The cross-section morphologies of SA control membrane and nanohybrid membranes were observed via SEM. It is shown in Figure 4a that the separation layer with the thickness of 232 ± 12 nm is tightly adhered to the PAN support layer. The SA control membrane exhibits smooth cross-section morphology (Figure 4b), while brick-and-mortar architectures appear after incorporating PSBMA@GO or GO (Figure 4c–f). The PSBMA@GO and GO nanosheets orient randomly in SA matrix under low content (Figure 4c and f). With the increase of loading content, more PSBMA@GO nanosheets are prone to aligning parallel to the membrane surface (Figure 4d and e). Both PSBMA@GO and GO were dispersed uniformly without apparent agglomeration in all the membranes.

Physical Structure of Nanohybrid Membranes. The free volume properties of SA control membrane and nanohybrid membranes were characterized by PALS as shown in Table 1. r_3 and I_3 are the radius and intensity of network pores, which mean the small cavities between polymer chains. r_4 and I_4

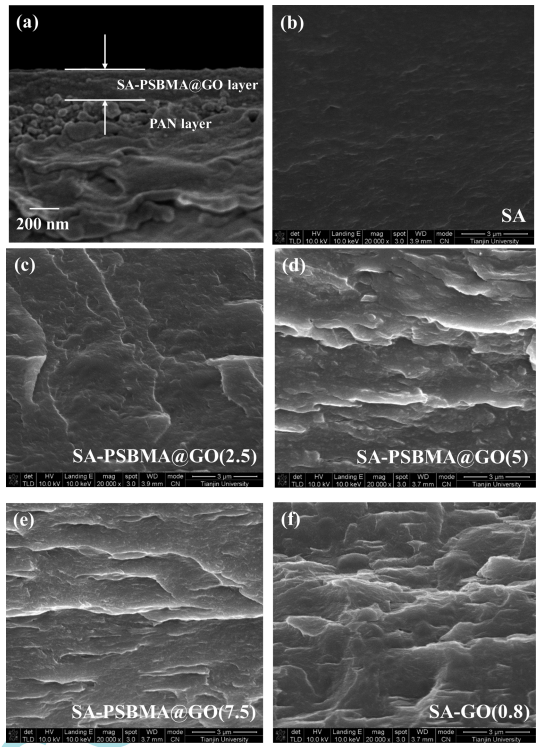

Figure 4. SEM images of the cross-section morphologies of (a) SA-PSBMA@GO(2.5)/PAN, (b) SA, (c) SA-PSBMA@GO(2.5), (d) SA-PSBMA@GO(5), (e) SA-PSBMA@GO(7.5), and (f) SA-GO(0.8).

Table 1. Free Volume Properties of SA Control Membrane and Nanohybrid Membranes

membrane	r_3 (nm)	I_3 (%)	r_4 (nm)	I_4 (%)	f_{app}
SA	0.129	13.31	0.287	5.59	0.215
SA-PSBMA@GO(2.5)	0.128	12.80	0.282	5.74	0.208
SA-PSBMA@GO(5)	0.147	11.78	0.305	4.19	0.210
SA-PSBMA@GO(7.5)	0.203	9.76	0.340	2.12	0.220
SA-GO(0.8)	0.195	11.07	0.332	2.47	0.229

are the radius and intensity of aggregate pores, including the larger spaces surrounding the polymer aggregates and the spaces at polymer-inorganic interface.[26] With the augment of PSBMA@GO content, both the radiuses of network pore and aggregate pore slightly diminish and then remarkably increase, while the intensities almost decrease all along. As a result, the fractional free volume (f_{app}) fluctuates in a narrow range. After incorporating PSBMA@GO, the electrostatic interactions between carboxyl groups on SA and quaternary ammonium group on SBMA restrict the mobility of SA chains, conferring the membrane with more compact structure and smaller free volume cavities. Meanwhile, the appearance of polymer–inorganic interface increases the aggregate pore intensity. At higher PSBMA@GO content, the restacking of nanosheets may occur, which brings multiple influences to the free volume properties of the polymer matrix, polymer-inorganic interface, and inorganic filler itself: (i) the interface area and interfacial interaction sites does not increase proportionally with PSBMA@GO content, leading to the reduced influence on polymer chains mobility; (ii) the two-dimensional PSBMA@GO can act as nucleating agent to induce the ordered arrangement of polymer chains on the surface of nanosheets, leading to the increased crystallinity in interface region; (iii)

DOI: 10.1021/acsami.5b10551
ACS Appl. Mater. Interfaces 2016, 8, 2097–2103

PSBMA@GO may bring free volume cavities between nanosheets. Compared with SA-GO(0.8) membrane, the SA-PSBMA@GO(2.5) membrane possesses free volume cavities with smaller size and higher intensity, arising from the different interfacial chemical compositions and interactions.

Separation Performance of Nanohybrid Membranes. To investigate the effect of incorporating PSBMA@GO on selective water-permeation, the pervaporation experiments of SA control membrane and nanohybrid membranes were performed with 90 wt % ethanol aqueous solution at 350 K. As shown in Figure 5a, both the permeation flux and separation

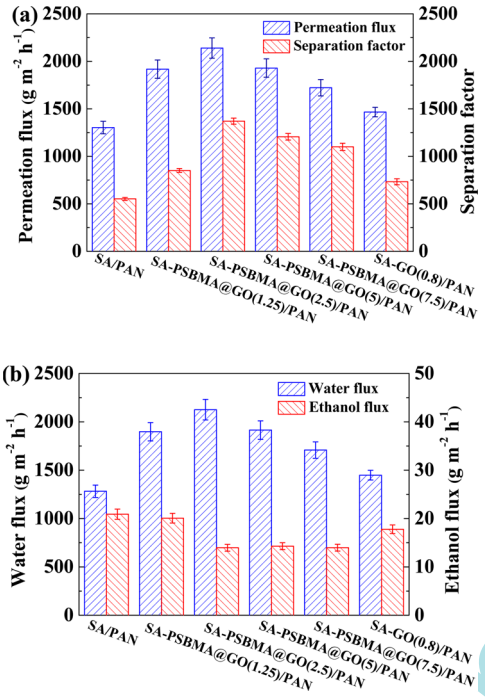

Figure 5. Pervaporation performance of SA control membrane and nanohybrid membranes: (a) permeation flux and separation factor and (b) water flux and ethanol flux.

factor of SA-PSBMA@GO/PAN membrane reach the maximum (with the permeation flux of 2140 g m^{-2} h^{-1} and the separation factor of 1370) when the content of PSBMA@GO is 2.5 wt %. Because the size of free volume cavities in SA-PSBMA@GO(2.5)/PAN membrane is similar to that of SA control membrane (Table 1), the influence of free volume on separation performance is negligible. Therefore, the enhancement of permeation flux and separation factor after incorporating PSBMA@GO is attributed to the introduction of zwitterionic pathway. The dense quaternary ammonium and sulfonate groups on PSBMA@GO surface bind abundant water molecules and then form hydration layer, which preferentially interacts with water molecules in feed solution and repels ethanol molecules, thus generating a specific and efficient water transport pathway on PSBMA@GO surface. As a result, the water flux augments while ethanol flux exhibits a reverse tendency when increasing the PSBMA@GO content as shown in Figure 5b. With the further increase of PSBMA@GO content, more PSBMA@GO nanosheets are prone to aligning parallel to the membrane surface, which prolongs the diffusion pathway of water and ethanol molecules. Meanwhile, the increscent size of free volume cavities weakens the molecular sieving effect for ethanol molecules. Consequently, the water flux declines while the ethanol flux almost keeps constant, leading to the decreased permeation flux and separation factor at higher PSBMA@GO content. Compared with SA-GO(0.8)/PAN membrane, higher permeation flux and separation factor are obtained for PSBMA@GO(0.8)/PAN membrane. The superior separation performance can be ascribed to three reasons: (i) the hydration layer on GO surface is induced mainly via hydrogen bond. Therefore, the water molecules outside the hydration layer on PSBMA@GO possess higher freedom and mobility compared with those outside the hydration layer on GO, which benefits water permeation; (ii) the higher ethanol repellency of PSBMA@GO compared with pristine GO endow the water transport pathway with higher selectivity; (iii) the SA-PSBMA@GO(2.5)/PAN membrane possesses free volume cavities with smaller size, which is in favor of the molecular sieving for ethanol molecules.

Figure 6 summarizes the performance of recently reported water/ethanol separation membranes with different kinds of

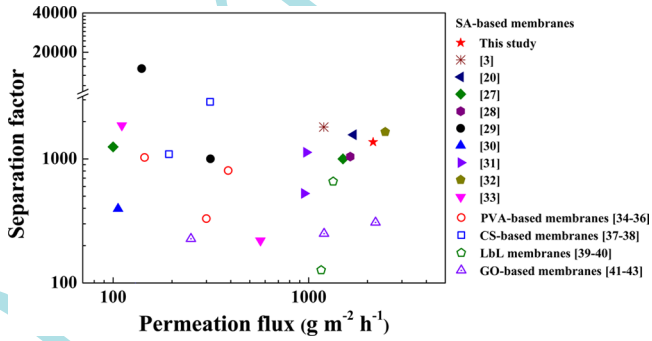

Figure 6. Comparison of the membrane in this study with recently reported membranes in literatures.[27−43]

materials (such as SA, poly(vinyl alcohol) (PVA), chitosan (CS), and grapheme oxide (GO)). The detailed information such as operation conditions, membrane thickness and PSI value is shown in Table S1. Because of the incorporation of zwitterionic water transport pathway on PSBMA@GO surface, the SA-PSBMA@GO/PAN nanohybrid membrane exhibits high permeation flux and desirable separation factor.

CONCLUSIONS

In this study, a novel approach to promoting the selective water-permeation across dense membrane was explored by constructing high-efficiency water transport pathway using zwitterionic GO nanosheets. Zwitterionic GO with high grafting-density (1.67 SBMA unit nm^{-2}) was prepared via free radical polymerization, and then incorporated into SA matrix to fabricate nanohybrid membrane. The membrane containing 2.5 wt % PSBMA@GO achieves the optimal separation performance with the permeation flux of 2140 g m^{-2} h^{-1} (164% of SA control membrane), and separation factor of 1370 (2.5 times of SA control membrane). Such superior separation performance arises from the combination of the optimized physical structure and chemical structure of water transport pathway: (i) the two-dimensional GO creates pathway with high level of continuity and (ii) the high-density zwitterionic groups on GO electrostatically induce dense and strong hydration layer, leading to high water affinity and ethanol repellency. Considering the pivotal role of water permeation in membrane field, this study may offer a generic and facile approach to preparing highly water-selective

DOI: 10.1021/acsami.5b10551
ACS Appl. Mater. Interfaces 2016, 8, 2097−2103

membranes for various dense membrane based separation processes.

■ ASSOCIATED CONTENT

Supporting Information

The Supporting Information is available free of charge on the ACS Publications website at DOI: 10.1021/acsami.5b10551.

Photographs of GO and PSBMA@GO dispersions with water or ethanol as solvent (Figure S1); TGA curves of GO and PSBMA@GO (Figure S2); static water contact angles on nanohybrid membrane surfaces (Figure S3); long-term separation performance of SA-PSBMA@GO(2.5)/PAN membrane (Figure S4); comparison of the membrane separation performance in this study with recently reported membranes in literatures (Table S1) (PDF)

■ AUTHOR INFORMATION

Corresponding Author

*Fax: +86 22 2350 0086. Tel: +86 22 2350 0086. E-mail: zhyjiang@tju.edu.cn.

Notes

The authors declare no competing financial interest.

■ ACKNOWLEDGMENTS

The authors are grateful to the financial support from the National Natural Science Foundation of China (21490583 and 21306131), the National Science Foundation for Distinguished Young Scholars (21125627), the Specialized Research Fund for the Doctoral Program of Higher Education (20120032120009), and the Program of Introducing Talents of Discipline to Universities (B06006).

■ REFERENCES

(1) Liang, B.; Zhan, W.; Qi, G. G.; Lin, S. S.; Nan, Q.; Liu, Y. X.; Cao, B.; Pan, K. High Performance Graphene Oxide/Polyacrylonitrile Composite Pervaporation Membranes for Desalination Applications. *J. Mater. Chem. A* **2015**, *3*, 5140−5147.

(2) Wu, D. H.; Huang, Y. F.; Yu, S. C.; Lawless, D.; Feng, X. S. Thin Film Composite Nanofiltration Membranes Assembled Layer-by-Layer via Interfacial Polymerization from Polyethylenimine and Trimesoyl chloride. *J. Membr. Sci.* **2014**, *472*, 141−153.

(3) Zhao, J.; Fang, C.; Zhu, Y.; He, G.; Pan, F.; Jiang, Z.; Zhang, P.; Cao, X.; Wang, B. Manipulating the Interfacial Interactions of Composite Membranes via a Mussel-Inspired Approach for Enhanced Separation Selectivity. *J. Mater. Chem. A* **2015**, *3*, 19980−19988.

(4) Geise, G. M.; Paul, D. R.; Freeman, B. D. Fundamental Water and Salt Transport Properties of Polymeric Materials. *Prog. Polym. Sci.* **2014**, *39*, 1−42.

(5) Wu, J.; Lin, W.; Wang, Z.; Chen, S.; Chang, Y. Investigation of the Hydration of Nonfouling Material Poly(Sulfobetaine Methacrylate) by Low-Field Nuclear Magnetic Resonance. *Langmuir* **2012**, *28*, 7436−7441.

(6) He, G.; Li, Z.; Zhao, J.; Wang, S.; Wu, H.; Guiver, M. D.; Jiang, Z. Nanostructured Ion-Exchange Membranes for Fuel Cells: Recent Advances and Perspectives. *Adv. Mater.* **2015**, *27*, 5280−5295.

(7) Shao, Q.; Jiang, S. Molecular Understanding and Design of Zwitterionic Materials. *Adv. Mater.* **2015**, *27*, 15−26.

(8) Jiang, S.; Cao, Z. Ultralow-Fouling, Functionalizable, and Hydrolyzable Zwitterionic Materials and Their Derivatives for Biological Applications. *Adv. Mater.* **2010**, *22*, 920−932.

(9) Xuan, F.; Liu, J. Preparation, Characterization and Application of Zwitterionic Polymers and Membranes: Current Developments and Perspective. *Polym. Int.* **2009**, *58*, 1350−1361.

(10) Leng, C.; Han, X.; Shao, Q.; Zhu, Y.; Li, Y.; Jiang, S.; Chen, Z. In Situ Probing of the Surface Hydration of Zwitterionic Polymer Brushes: Structural and Environmental Effects. *J. Phys. Chem. C* **2014**, *118*, 15840−15845.

(11) He, G. W.; Li, Z. Y.; Li, Y. F.; Li, Z.; Wu, H.; Yang, X. L.; Jiang, Z. Y. Zwitterionic Microcapsules as Water Reservoirs and Proton Carriers within a Nafion Membrane to Confer High Proton Conductivity under Low Humidity. *ACS Appl. Mater. Interfaces* **2014**, *6*, 5362−5366.

(12) Liu, Y.; Peng, D. D.; He, G. W.; Wang, S. F.; Li, Y. F.; Wu, H.; Jiang, Z. Y. Enhanced CO_2 Permeability of Membranes by Incorporating Polyzwitterion@CNT Composite Particles into Polyimide Matrix. *ACS Appl. Mater. Interfaces* **2014**, *6*, 13051−13060.

(13) Chou, Y. N.; Chang, Y.; Wen, T. C. Applying Thermosettable Zwitterionic Copolymers as General Fouling-Resistant and Thermal-Tolerant Biomaterial Interfaces. *ACS Appl. Mater. Interfaces* **2015**, *7*, 10096−10107.

(14) Zhao, J.; Zhao, X. T.; Jiang, Z. Y.; Li, Z.; Fan, X. C.; Zhu, J. A.; Wu, H.; Su, Y. L.; Yang, D.; Pan, F. S.; Shi, J. F. Biomimetic and Bioinspired Membranes: Preparation and Application. *Prog. Polym. Sci.* **2014**, *39*, 1668−1720.

(15) Zhao, X. Z.; He, C. J. Efficient Preparation of Super Antifouling PVDF Ultrafiltration Membrane with One Step Fabricated Zwitterionic Surface. *ACS Appl. Mater. Interfaces* **2015**, *7*, 17947−17953.

(16) Wang, J.; Wang, Z.; Wang, J.; Wang, S. Improving the Water Flux and Bio-Fouling Resistance of Reverse Osmosis (RO) Membrane through Surface Modification by Zwitterionic Polymer. *J. Membr. Sci.* **2015**, *493*, 188−199.

(17) Ni, L.; Meng, J.; Geise, G. M.; Zhang, Y.; Zhou, J. Water and Salt Transport Properties of Zwitterionic Polymers Film. *J. Membr. Sci.* **2015**, *491*, 73−81.

(18) Dreyer, D. R.; Todd, A. D.; Bielawski, C. W. Harnessing the Chemistry of Graphene Oxide. *Chem. Soc. Rev.* **2014**, *43*, 5288−5301.

(19) Liu, G. P.; Jin, W. Q.; Xu, N. P. Graphene-Based Membranes. *Chem. Soc. Rev.* **2015**, *44*, 5016−5030.

(20) Cao, K.; Jiang, Z.; Zhao, J.; Zhao, C.; Gao, C.; Pan, F.; Wang, B.; Cao, X.; Yang, J. Enhanced Water Permeation through Sodium Alginate Membranes by Incorporating Graphene Oxides. *J. Membr. Sci.* **2014**, *469*, 272−283.

(21) Shen, J.; Hu, Y.; Li, C.; Qin, C.; Shi, M.; Ye, M. Layer-by-Layer Self-assembly of Graphene Nanoplatelets. *Langmuir* **2009**, *25*, 6122−6128.

(22) Kan, L.; Xu, Z.; Gao, C. General Avenue to Individually Dispersed Graphene Oxide-Based Two-Dimensional Molecular Brushes by Free Radical Polymerization. *Macromolecules* **2011**, *44*, 444−452.

(23) Zhao, J.; Zhu, Y. W.; Pan, F. S.; He, G. W.; Fang, C. H.; Cao, K. T.; Xing, R. S.; Jiang, Z. Y. Fabricating Graphene Oxide-Based Ultrathin Hybrid Membrane for Pervaporation Dehydration via Layer-by-Layer Self-Assembly Driven by Multiple Interactions. *J. Membr. Sci.* **2015**, *487*, 162−172.

(24) Nagel, C.; Gunther, S. K.; Fritsch, D.; Strunskus, T.; Faupel, F. Free Volume and Transport Properties in Highly Selective Polymer Membranes. *Macromolecules* **2002**, *35*, 2071−2077.

(25) He, G. W.; Chang, C. Y.; Xu, M. Z.; Hu, S.; Li, L. Q.; Zhao, J.; Li, Z.; Li, Z. Y.; Yin, Y. H.; Gang, M. Y.; Wu, H.; Yang, X. L.; Guiver, M. D.; Jiang, Z. Y. Tunable Nanochannels along Graphene Oxide/Polymer Core-Shell Nanosheets to Enhance Proton Conductivity. *Adv. Funct. Mater.* **2015**, *25*, 7502.

(26) Zhao, J.; Ma, J.; Chen, J.; Pan, F. S.; Jiang, Z. Y. Experimental and Molecular Simulation Investigations on Interfacial Characteristics of Gelatin/Polyacrylonitrile Composite Pervaporation Membrane. *Chem. Eng. J.* **2011**, *178*, 1−7.

(27) Magalad, V. T.; Gokavi, G. S.; Ranganathaiah, C.; Burshe, M. H.; Han, C.; Dionysiou, D. D.; Nadagouda, M. N.; Aminabhavi, T. M. Polymeric Blend Nanocomposite Membranes for Ethanol Dehydration-Effect of Morphology and Membrane-Solvent Interactions. *J. Membr. Sci.* **2013**, *430*, 321−329.

DOI: 10.1021/acsami.5b10551
ACS Appl. Mater. Interfaces 2016, 8, 2097−2103

(28) Zhao, C. H.; Jiang, Z. Y.; Zhao, J.; Cao, K. T.; Zhang, Q.; Pan, F. S. High Pervaporation Dehydration Performance of the Composite Membrane with an Ultrathin Alginate/Poly(acrylic acid)-Fe_3O_4 Active Layer. *Ind. Eng. Chem. Res.* **2014**, *53*, 1606−1616.
(29) Magalad, V. T.; Supale, A. R.; Maradur, S. P.; Gokavi, G. S.; Aminabhavi, T. M. Preyssler Type Heteropolyacid-Incorporated Highly Water-Selective Sodium Alginate-Based Inorganic-Organic Hybrid Membranes for Pervaporation Dehydration of Ethanol. *Chem. Eng. J.* **2010**, *159*, 75−83.
(30) Nigiz, F. U.; Dogan, H.; Hilmioglu, N. D. Pervaporation of Ethanol/Water Mixtures Using Clinoptilolite and 4A Filled Sodium Alginate Membranes. *Desalination* **2012**, *300*, 24−31.
(31) Gao, C. Y.; Zhang, M. H.; Ding, J. W.; Pan, F. S.; Jiang, Z. Y.; Li, Y. F.; Zhao, J. Pervaporation Dehydration of Ethanol by Hyaluronic Acid/Sodium Alginate Two-Active-Layer Composite Membranes. *Carbohydr. Polym.* **2014**, *99*, 158−165.
(32) Cao, K.; Jiang, Z.; Zhang, X.; Zhang, Y.; Zhao, J.; Xing, R.; Yang, S.; Gao, C.; Pan, F. Highly Water-Selective Hybrid Membrane By Incorporating g-C_3N_4 Nanosheets into Polymer Matrix. *J. Membr. Sci.* **2015**, *490*, 72−83.
(33) Adoor, S. G.; Rajineekanth, V.; Nadagouda, M. N.; Rao, K. C.; Dionysiou, D. D.; Aminabhavi, T. M. Exploration of Nanocomposite Membranes Composed of Phosphotungstic Acid in Sodium Alginate for Separation of Aqueous-Organic Mixtures by Pervaporation. *Sep. Purif. Technol.* **2013**, *113*, 64−74.
(34) Panahian, S.; Raisi, A.; Aroujalian, A. Multilayer Mxed Mtrix Mmbranes Containing Mdified-MWCNTs for Dhydration of Acohol by Prvaporation Pocess. *Desalination* **2015**, *355*, 45−55.
(35) Xia, L. L.; Li, C. L.; Wang, Y. In-situ Crosslinked PVA/Organosilica Hybrid Membranes for Pervaporation Separations. *J. Membr. Sci.* **2016**, *498*, 263−275.
(36) Li, G. H.; Shi, L.; Zeng, G. F.; Li, M.; Zhang, Y. F.; Sun, Y. H. Sharp Molecular-Sieving of Alcohol-Water Mixtures over Phenyldiboronic Acid Pillared Graphene Oxide Framework (GOF) Hybrid Membrane. *Chem. Commun.* **2015**, *51*, 7345−7348.
(37) Dharupaneedi, S. P.; Anjanapura, R. V.; Han, J. M.; Aminabhavi, T. M. Functionalized Graphene Sheets Embedded in Chitosan Nanocomposite Membranes for Ethanol and Isopropanol Dehydration via Pervaporation. *Ind. Eng. Chem. Res.* **2014**, *53*, 14474−14484.
(38) Kang, C. H.; Lin, Y. F.; Huang, Y. S.; Tung, K. L.; Chung, K. S.; Chen, J. T.; Hung, W. S.; Lee, K. R.; Lai, J. Y. Synthesis of ZIF-7/Chitosan Mixed-Matrix Membranes with Improved Separation Performance of Water/Ethanol Mixtures. *J. Membr. Sci.* **2013**, *438*, 105−111.
(39) Shi, G. M.; Zuo, J.; Tang, S. H.; Wei, S.; Chung, T. S. Layer-by-Layer (LbL) Polyelectrolyte Membrane with Nexar™ Polymer as a Polyanion for Pervaporation Dehydration of Ethanol. *Sep. Purif. Technol.* **2015**, *140*, 13−22.
(40) Zhao, J.; Pan, F. S.; Li, P.; Zhao, C. H.; Jiang, Z. Y.; Zhang, P.; Cao, X. Z. Fabrication of Ultrathin Membrane via Layer-by-Layer Self-assembly Driven by Hydrophobic Interaction Towards High Separation Performance. *ACS Appl. Mater. Interfaces* **2013**, *5*, 13275−13283.
(41) Yeh, T. M.; Wang, Z.; Mahajan, D.; Hsiao, B. S.; Chu, B. High Flux Ethanol Dehydration Using Nanofibrous Membranes Containing Graphene Oxide Barrier Layers. *J. Mater. Chem. A* **2013**, *1*, 12998−13003.
(42) Tang, Y. P.; Paul, D. R.; Chung, T. S. Free-Standing Graphene Oxide Thin Films Assembled by a Pressurized Ultrafiltration Method for Dehydration of Ethanol. *J. Membr. Sci.* **2014**, *458*, 199−208.
(43) Li, G. H.; Shi, L.; Zeng, G. F.; Zhang, Y. F.; Sun, Y. H. Efficient Dehydration of the Organic Solvent through Graphene Oxide (GO)/Ceramic Composite Membranes. *RSC Adv.* **2014**, *4*, 52012−52015.

DOI: 10.1021/acsami.5b10551
ACS Appl. Mater. Interfaces 2016, 8, 2097−2103